

We are IntechOpen, the world's leading publisher of Open Access books Built by scientists, for scientists

6,900

Open access books available

185,000

International authors and editors

200M

Downloads

Our authors are among the

154

Countries delivered to

TOP 1%

most cited scientists

12.2%

Contributors from top 500 universities



WEB OF SCIENCE™

Selection of our books indexed in the Book Citation Index
in Web of Science™ Core Collection (BKCI)

Interested in publishing with us?
Contact book.department@intechopen.com

Numbers displayed above are based on latest data collected.
For more information visit www.intechopen.com



Application of Kalman Filter and Breeding Ensemble Technique to Forecast the Tropical Cyclone Activity

Cong Thanh, Dao Nguyen Quynh Hoa and Tran Tan Tien

Abstract

Tropical cyclone (TC) is one of the major meteorology disasters, as they lead to deaths, destroy the infrastructure and the environment. Therefore, how to improve the predictability of TC's activities, such as formation, track, and intensity, is very important and is considered an important task for current operational predicting TC centers in many countries. However, predicting TC's activities has remained a big challenge for meteorologists due to our incomplete understanding of the multiscale interaction of TCs with the ambient environment and the limitation of numerical weather forecast tools. Hence, this chapter will exhibit some techniques to improve the ability to predict the formation and track of TCs using an ensemble prediction system. Particularly, the Local Ensemble Transform Kalman Filter (LETKF) scheme and its implementation in the WRF Model, as well as the Vortex tracking method that has been applied for the forecast of TCs formation, will be presented in subSection 1. Application of Breeding Ensemble to Tropical Cyclone Track Forecasts using the Regional Atmospheric Modeling System (RAMS) model will be introduced in subSection 2.

Keywords: The WRF-LETKF system, Ensemble forecast technique, Breeding Ensemble, data assimilation system, Tropical cyclone forecast

1. Introduction

1.1 The forecast of TCs formation using the ensemble Kalman filter

Among several approaches for real-time monitoring and forecasting of TC formation, direct numerical products from global and regional weather prediction models appear to be the most reliable at present, despite their inherent limitations and uncertainties (e.g., see [1, 2]). The skillful performance of TC formation forecasts by numerical models has been well documented in many previous studies [3–8]. This achievement of numerical models is attributed to a variety of advanced research on upgrading parameterizations of physics, resolution, computational resources, and data assimilation schemes [1, 9]. Among several different assimilation schemes, the ensemble Kalman filter (EnKF) has been extensively applied to many practical problems in recent years due to its straightforward implementation for TC forecast applications [10–16]. The use of EnKF for TC forecasting applications is increasingly

popular, given the current availability of real-time flight reconnaissance data that allows direct assimilation of airborne observations without the need of a bogus vortex (e.g., see [10, 14–16]). In essence, the development of EnKF addressed the problem when using variational assimilation schemes in which the background covariance matrix is allowed to be time-dependent. Hence, the model would adapt better with fast-evolving and complicated dynamical systems such as TCs or mesoscale convective systems [12, 17–19]. There is an efficient method of implementing an Ensemble Kalman Filter (EnKF), which was called a Local Ensemble Transform Kalman Filter (LETKF) scheme.

1.2 Data assimilation system

In this section, the LETKF algorithm proposed by Ott et al. [20] and Hunt et al. [21] is adopted and implemented for the WRF Model. The primary usage of the LETKF algorithm is utilizing the background ensemble matrix as an operator to transform state vectors from a model space spanned by the model grid points within a local patch to an ensemble space spanned by ensemble members. The procedures for calculating matrix and generating the ensemble analyses are executed in this low dimension ensemble space at every single grid point. In this sense, the LETKF scheme allows the ensemble space to be performed locally and in parallel efficiently for practical problems, especially when carrying out a large-volume of data (e.g., see [8, 11, 12, 22–25]).

With its promising capability, LETKF has been implemented in the WRF Model (V3.6, hereafter referred to as the WRF-LETKF system). With an aim to practical forecasting applications, all the observations utilizing in the WRF – LETKF scheme are preprocessing in a quality control taken by the WRF data assimilation (WRFDA) component. In addition, the WRFDA component also generates lateral boundary conditions for each ensemble member once obtained the analysis update. Hence, each ensemble member possesses its own boundary dynamically consistent with its own updated initial conditions. More details in the WRF-LETKF design can be found in [12, 24]. The focal point here is how the ensembles with and without augmented observations perform. In this regard, the relative differences in the output among these ensembles can derive the main effects of additional augmented observations.

To begin the ensemble system, a first-guess background is generated in a cold-start ensemble by first using 3DVAR scheme to produce an analysis from a GFS initial condition. Random perturbations with standard deviations of 1 ms^{-1} for the wind field, 1 K for temperature, and $1 \times 10^{-3} \text{ kg kg}^{-1}$ for specific humidity at all model grid points are then added to the 3DVAR-generated analyses for the cold-start ensemble. The 3DVAR-generated analyses as initial conditions for 12-h running in a manner that the outputs from these 12-h integrations can be subsequently used as a *warm-start* background for the LETKF ensemble assimilation in the next cycle. Note that these random perturbations are added only for the first cold-start cycle to create a background ensemble. All subsequent warm-run cycles use the WRF-LETKF 12-h forecasts as a background ensemble and so no additional random noises are necessary. The newly generated analysis perturbation ensemble at each cycle is then added to the GFS analysis to produce the next ensemble initial conditions when run in the cycling mode as described in [26].

1.3 The LETKF algorithm

To get a better understanding of the LETKF algorithm mentioned in the previous sub-section. A brief description of this LETKF algorithm that developed by Kieu et al. [12] has been presented below:

Assume that give a background ensemble $\{\mathbf{x}^{b(i)}: i = 1, 2, \dots, k\}$, where k is the number of ensemble members (assuming that the analysis is taken one at a time, so the time index is not included). According to Hunt et al. [21], an ensemble mean $\bar{\mathbf{x}}^b$ and an ensemble perturbation matrix \mathbf{X}^b are defined respectively as:

$$\bar{\mathbf{x}}^b = \frac{1}{k} \sum_{i=1}^k \mathbf{x}^{b(i)}.$$

$$\mathbf{X}^b = \left\{ \mathbf{x}^{b(1)} - \bar{\mathbf{x}}^b, \mathbf{x}^{b(2)} - \bar{\mathbf{x}}^b, \dots, \mathbf{x}^{b(k)} - \bar{\mathbf{x}}^b \right\}. \quad (1)$$

Let $\mathbf{x} = \bar{\mathbf{x}}^b + \mathbf{X}^b \mathbf{w}$, where \mathbf{w} is a local vector in the ensemble space, the local cost function to be minimized in the ensemble space is given by:

$$\hat{j}(\mathbf{w}) = (k-1) \mathbf{w}^T \left\{ \mathbf{I} - (\mathbf{X}^b)^T \left[\mathbf{X}^b (\mathbf{X}^b)^T \right]^{-1} \mathbf{X}^b \right\} \mathbf{w} + J[\bar{\mathbf{x}}^b + \mathbf{X}^b \mathbf{w}], \quad (2)$$

Where $J[\bar{\mathbf{x}}^b + \mathbf{X}^b \mathbf{w}]$ is the cost function in the model space. If one defines the null space of \mathbf{X}^b as $N = \{\mathbf{v} | \mathbf{X}^b \mathbf{v} = 0\}$, then the cost function $\hat{j}(\mathbf{w})$ is divided into two parts: one containing the component of \mathbf{w} in N (the first term in Eq. (2)), and the second depending on the components of \mathbf{w} that are orthogonal to N . By requiring that the mean analysis state $\bar{\mathbf{w}}^a$ is orthogonal to N such that the cost function $\hat{j}(\mathbf{w})$ is minimized, the mean analysis state and its corresponding analysis error covariance matrix in the ensemble space can be found as:

$$\bar{\mathbf{w}}^a = \hat{\mathbf{P}}^a (\mathbf{Y}^b)^T \mathbf{R}^{-1} [\mathbf{y}^0 - \mathbf{H}(\bar{\mathbf{x}}^b)] \quad (3)$$

$$\hat{\mathbf{P}}^a = \left[(k-1) \mathbf{I} + (\mathbf{Y}^b)^T \mathbf{R}^{-1} \mathbf{Y}^b \right]^{-1}, \quad (4)$$

Where $\mathbf{Y}^b \equiv \mathbf{H}(\mathbf{x}^{b(i)} - \bar{\mathbf{x}}^b)$ is the ensemble matrix of background perturbations valid at the observation locations, and \mathbf{R} is the observational error covariance matrix. By noting that the analysis error covariance matrix \mathbf{P}^a in the model space and $\hat{\mathbf{P}}^a$ in the ensemble space have a simple connection of $\mathbf{P}^a = \mathbf{X}^b \hat{\mathbf{P}}^a (\mathbf{X}^b)^T$, the analysis ensemble perturbation matrix \mathbf{X}^a can be chosen as follows:

$$\mathbf{X}^a = \mathbf{X}^b \left[(k-1) \hat{\mathbf{P}}^a \right]^{1/2}. \quad (5)$$

The analysis ensemble \mathbf{x}^a is finally obtained as:

$$\mathbf{x}^{a(i)} = \bar{\mathbf{x}}^b + \mathbf{X}^b \left\{ \bar{\mathbf{w}}^a + \left[(k-1) \hat{\mathbf{P}}^{a(i)} \right]^{1/2} \right\}. \quad (6)$$

Detailed handling of more general nonlinear and synchronous observations in LETKF can be found in [21]. It should be noticed that the above formulas are only valid without model errors. To take into account the model errors, Hunt et al. [21] suggested that a multiplicative factor should be introduced in Eq. (4) (specifically, the first factor on the right hand side of Eq. (4)). This simple additional multiplicative inflation is easy to implement in the scheme, and has been shown to be efficient in many applications of the LETKF (e.g., see [25, 27, 28]).

1.4 Vortex tracking method

Constructing a suitable vortex-tracking algorithm is a must-have procedure to detect the formation of a newly developed TC center in all ensemble members since their outputs are diverse. A good detection scheme allows one to define and verify the location and the timing of TC formation centers. This step is crucial in every TC formation study, due to the difficulties in capturing the incoherent structure of tropical cyclones at the early genesis stages. More precisely, one cannot apply general criteria such as a midlevel warm-core anomaly, maximum vorticity center for the tropical disturbances as for mature TCs. Instead, the early formation of a tropical depression is often imprinted by the existence of an upper-level cold core and/or a weak surface low pressure rather than a midlevel warm core (see, e.g., [29, 30]). Thus, very few conditions can be practically applied to detect a formation center during the genesis stage. To detect TC formation centers for real-time forecast, a simple scheme has been built upon standard conditions related to the maximum surface wind and the minimum central pressure, as follows:

First, the minimum sea level pressure P_{\min} within the study area is searched at every model grid point of each ensemble member output at each forecast lead time. Any location with $P_{\min} < 1004$ hPa will be noted down as a potential candidate for TC formation location at that forecast lead time for that particular ensemble member.

Second, once a possible location of TC formation is defined, the maximum 10-m wind speed V_{\max} in an area of $4^\circ \times 4^\circ$ surrounding the minimum pressure center is checked and recorded. A TC formation center will be marked if the condition $V_{\max} \geq 10 \text{ ms}^{-1}$ is satisfied. It is noteworthy that this value is considerably smaller than the global definition of a tropical depression wind speed ($\sim 17 \text{ ms}^{-1}$), due to the relatively coarse 27–/9-km resolution configuration of WRF-LETKF system. Visualizing verification of each TC circulation center detected based on this threshold proves that these criteria can properly identify the center of tropical cyclone like vortex during the genesis stage. Therefore, this threshold for V_{\max} is used for all genesis analyses. In fact, these criteria of tracking TC formation centers are somewhat intuitive and require further verification. However, this approach is acceptable in evaluating the augmented observational data impacts on TC formation forecasts among ensemble forecasts. As long as the tracking scheme remains certain in all analyses, the comparison of TC formation forecasts should answer the question about the performance of augmented observations in ensemble forecasts.

1.4.1 Example 1

The WRF-LETKF (WRF V3.6) system has been applied to study the formation of Typhoon Wutip. With target is to evaluate the sensitivity of TC formation forecast to different types of augmented observations. The WRF-LETKF system is designed in such a way that all observations are subject to quality control by the WRF data assimilation (WRFDA) component before used by the LETKF algorithm (More details about the implementation of the WRF-LETKF design can be found in [12, 22]. There is a total of 21 ensemble members was made (due to limited computational and storage resources) and all ensemble experiments are integrated for three days starting from 1200 UTC 23 September, which is approximately 48 h before a tropical depression precursor of Wutip was first reported in the TC vital record at 1200 UTC 25 September. The multiple physical schemes have been used in categorizing among ensemble experiments are 1) two cumulus parameterization schemes including the Betts–Miller–Janjic’ (BMJ) cumulus parameterization and the Kain–Fritsch with shallow convection schemes, 2) three planetary boundary

layer (PBL) parameterization schemes including the Yonsei University, the Mellor–Yamada–Janjic’, and the simple Medium-Range Forecast (MRF) schemes, 3) three microphysical schemes including the WSM 3 microphysics, the Kessler, and the Lin et al. schemes; and 4) two longwave radiative schemes including the Dudhia and the Goddard schemes for both longwave and shortwave radiations. The cold start cycle is therefore initialized at 0000 UTC 23 September to generate a background ensemble for the first-guess cycle at 1200 UTC 23 September. Afterwards, the subsequent cycles are implemented at every 6 h from 1200 UTC 23 September to 1200 UTC 26 September.

The augmented observational data used in the WRF-LETKF assimilation scheme include two main sources. The first is the satellite data (CIMSS-AMV) derived atmospheric motion vector (AMV) data maintained by the Cooperative Institute for Meteorological Satellite Studies (CIMSS), University of Wisconsin [21, 31–34] due to this data covers a large area where TC genesis may take place. The second source of local augmented observations in the domain of influence to Vietnam’s coastal region (DOIV) is also used, including 96 aviation routine weather (METAR) reports from routine scheduled observations, 31 ship/buoy (SHIP/BUOY) station reports, 59 enhanced sounding stations (SOUND), and 404 surface synoptic observations (SYNOP) reports of weather observations during the 0000 UTC 24 September–0000 UTC 27 September period.

Results show critical impacts of the (CIMSS-AMV) data in improving the large – scale environment favorable or hostile to the formation of Typhoon Wutip among ensemble members, which is dynamically controlled by monsoon trough. The results show the optimality of data impacts at cycle 36 h prior to Wutip’s observed formation and decrease as forecast cycles are closer to formation period. In contrast, the data assimilation with only surface and local station data proves that these source data are not enough to help describe the strength of monsoon trough due to their scattered distributions (**Figures 1–3**).

By choosing Typhoon Wutip as a case study, it was demonstrated that the initial conditions for tropical cyclogenesis in large-scale monsoon trough environment are sensitive to augmented observations. It could allow a range of outcomes for timing and location predictability of TC formation, especially at 36-hr cycle ensemble. Our results could present the importance of augmented observations, especially the

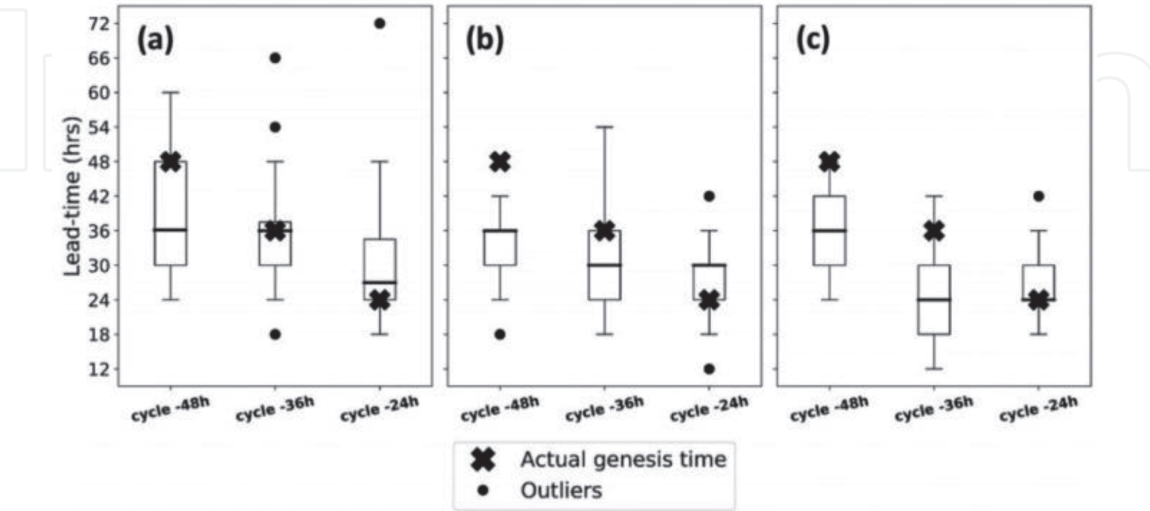


Figure 1. Boxplots of the timing for Wutip formation for three consecutive cycles 1200 UTC 23 Sep, 0000 UTC 24 Sep, and 1200 UTC 24 Sep, corresponding to 48, 36, and 24 h prior to the formation of Wutip depression for (a) the WRF-LETKF, (b) assimilation without the CIMSS-AMV data (NAMV), and (c) the GFS initial data [hereafter to as no data assimilation (NDA) ensemble]. The bold cross denotes the actual time that Wutip first became a tropical depression at 1200 UTC 25 Sep [35].

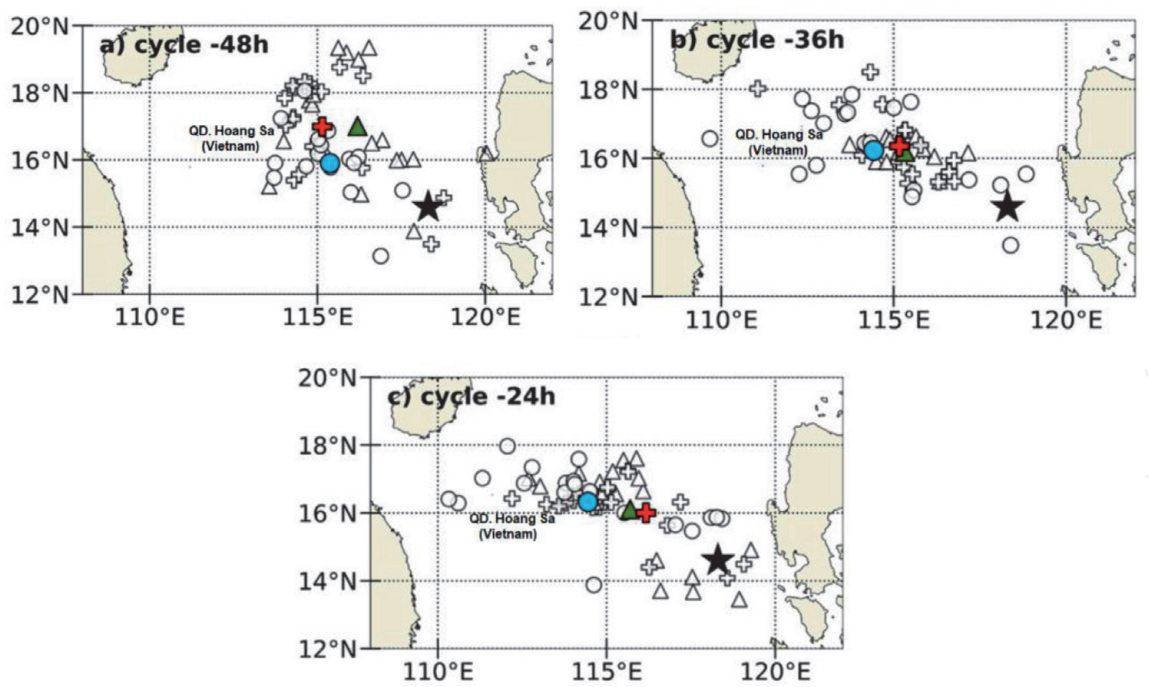


Figure 2. Distribution of the location of the Wutip’s formation centers as forecast by the WRF-LETKF (triangle), the assimilation without the CIMSS-AMV data ensemble (circle), and no data assimilation ensemble (cross) for (a) 48-, (b) 36-, and (c) 24-h cycles. Color symbols denote the ensemble means of corresponding forecasts [35].

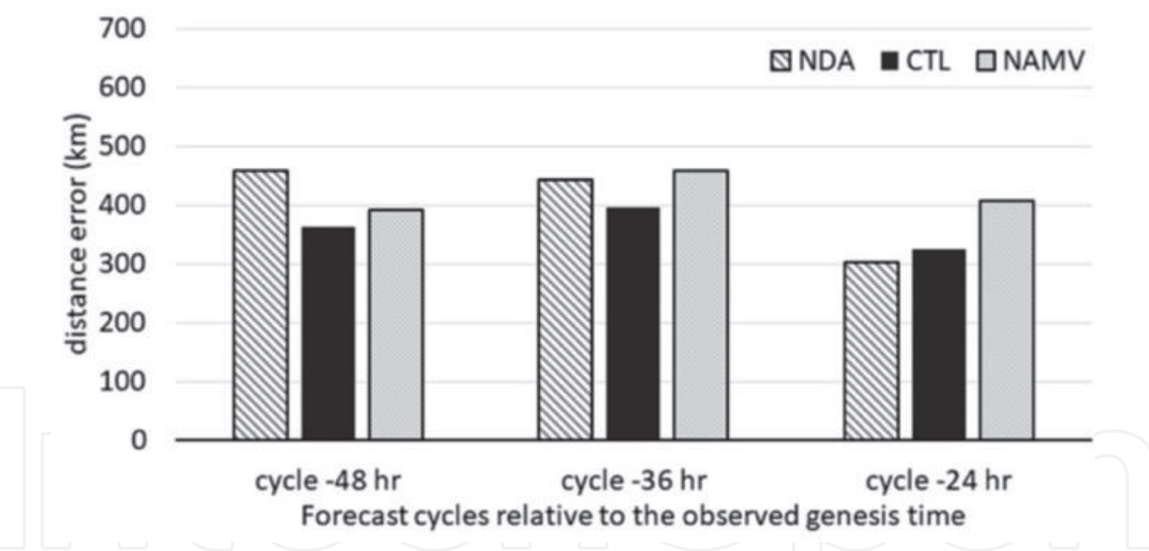


Figure 3. Ensemble mean distance errors between the forecasted and observed location of Wutip’s formation reported at 1200 UTC 25 Sep for three cycles of 48, 36, and 24 h obtained from the WRF-LETKF forecast (black), NDA forecast (stripe), and NAMV forecasts (light shaded) [35].

satellite AMV data, for the prediction of TC formation at certain lead times that are vital for operational TC forecasts. This case study is typical for TC formation in the WPAC basin, but not representative and may not be applied to other tropical cyclogenesis pathways. While WRF-LETKF has been utilized in forecasting tropical cyclogenesis in the marsupial paradigm of African Easterly Wave [36, 37], it has not been focused in the physical mechanisms of TCs formation in the BIEN DONG basin before. Wutip’s formation is strongly rooted in the monsoon trough, as most of the tropical cyclones in the BIEN DONG form within this pattern per year. The performance of WRF-LETKF with augmented observations in this case study has

innovated to the upcoming studies in more properly general examination when designing future observing systems.

2. Application of breeding ensemble to tropical cyclone track forecasts

2.1 Background

With limited range of predictability at the convective scale and short timescale and the complex variation of nature, predicting tropical cyclone (TC) tracks and intensity is one specific example that demonstrates vividly the sensitivity of numerical models to uncertainties in the atmosphere [26, 38, 39]. The inherent uncertainties associated with our current incomplete understanding of model physical processes or numerical approximations often lead to large errors in track and intensity forecast, especially at the lead times longer 3 days or under circumstances interacting with uneven terrain or complicated vortex mergers [40–42]. Currently, the US Joint Typhoon Warning Center (JTWC) showed that the official track errors in the North Western Pacific (WPAC) basin are as high as 220 km at 3-day estimation and 450 km at 5-day estimation. Likewise, the intensity forecast errors make no headway since no significant update was taken at all forecast ranges during the last 30 years. The recent effort to calculate uncertainty in TC forecasts is based on the ensemble prediction systems. Generally, there are 3 major special techniques to develop an ensemble forecast system include: (1) use the different initial conditions obtained from a posterior analysis error distribution (the Monte-Carlo ensembles) for one specific model, (2) Use a single initial condition for multiple different prediction models; and (3) use combine both dissimilar initial conditions and different prediction models.

The breeding ensemble approach in the first direction was first implemented in the operational Global Forecasting System (GFS) at the National Center for Environmental Prediction (NCEP, by Toth and Kalnay in 1993 and 1997 [43, 44], hereinafter TK93 and TK97, respectively) in 1993, and then became more popular and more applied in practice. The breeding method continuously employed previous cycles to calculate the fastest growing instabilities and then normalized these errors vectors into the so-called the bred vectors. This procedure could allow projecting the fastest growing modes onto the calculated bred vectors in a shade of perturbations in each breeding cycle. Likewise, a similar ensemble forecasting technique generating singular vectors instead of bred vectors is implemented in the European Center for medium-term weather forecast (ECMWF) in early 1992 [45, 46]. Although theoretically, the fastest growing modes should be projected onto bred vectors (at the far limit of the backward Lyapunov vectors), the experimental results retrieved from the TK93's breeding method indicate that the produced TC ensemble tracks could be very similar to each other, i.e., the spread of the system was relatively narrow (**Figure 4**). One possible explanation for such small ensemble dispersion is because the bred vectors collapsed into a similar dominant direction after several cycles, which is not an uncommon issue (e.g., see [48, 49]). The singular vectors display the fastest growing modes in terms of orthogonal directions within a short-range interval (via a tangential linear model). In contrast, the bred vectors are some extent equivalent to the leading Lyapunov vectors in a nonlinear finite-amplitude method [43, 50]. This method allows the bred vectors collapsing afterwards, and becoming linearly independent (non-orthogonal) in the presence of the lower dimension attractor [48, 51].

By consider both the spatial-temporal variations of the scaling vector at each cycle, the bred vectors could capture the local growing directions and thus allow for

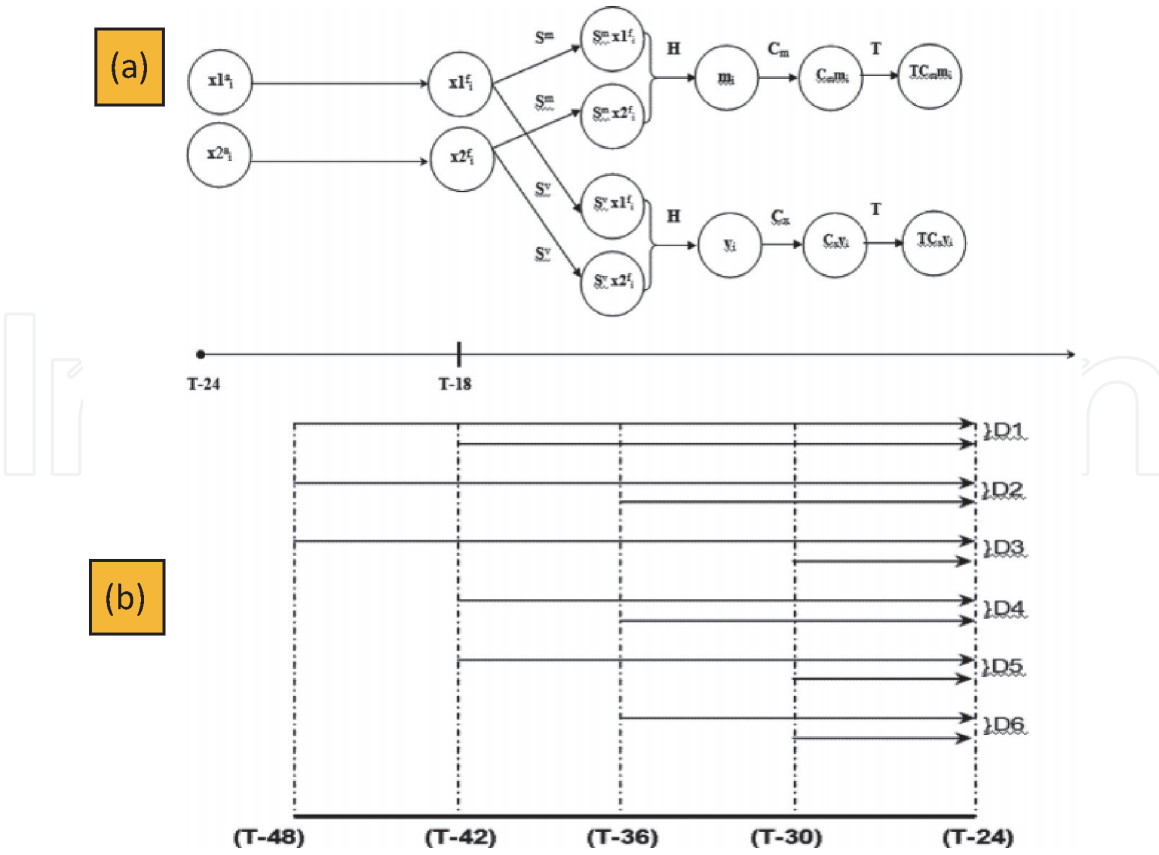


Figure 4. Schematic design of the TC-breeding ensemble technique: a) illustration of generating environmental bred vectors and TC bred vectors during a warm start cycle (from 24 h to 18 h before the target forecast date) b) illustration of making six pairs of lagged-averaged forecast (LAF) vectors for the first cold start cycle used in the TC-breeding ensemble [47].

larger ensemble spread [44, 52]. However, fast convective instabilities still quickly saturate after several breeding cycles, especially within the region where the atmospheric dynamics are complicated [53, 54]. Unfortunately, the TCs system act as such complicated phenomenon with multi-scale interactions. It is expected that the instability within the storm's inner-core should behave differently as compared to the outer environmental region. Previous studies (see [55– 57]) indicated that perturbations inside the TC inner-core area often develop and propagate rapidly in the manner of vortex Rossby waves with typical time scale of 12–24 h. Contrarily, the large-scale environmental related-perturbations propagate in a much smaller time scale, often manifested in terms of gravity waves and mesoscale clustering along the most unstable regions [58]. Representing the interaction between the faster storm-scale instabilities and slower large-scale environment is a big challenge in constructing an ensemble breeding system for TC forecasts. Hence, this section presented a new TC breeding approach that could help improve this challenge.

2.2 TC breeding method

Though the first breeding method presented by TK93 could capture the trend of fastest-growing during a finite time window, the real world TCs have a finite life cycle. Due to the high-resolution regional modeling required large computation, TC predicting models are typically spark off only when their TCs are already first reported in the warning centers, because it is a challenge to conserve a continuous ensemble of breeding cycles with taking much computational capacity for a long time. Therefore, TK93's breeding scheme could not instantaneously acquire

directions of most unstable modes during the earliest cycles. Moreover, utilizing only single re-scaling factor for both storm inner-core region and ambient environment with distinguished spatio-temporal scales does not enclose all mesoscale unstable nodes associated with TC vortex dynamics for which perturbations at different spatial-temporal scales grow at different rates [59]. Hence, it is necessary to change the rescaling factors following both the flow and the scales of instabilities [13].

Since our TC-breeding approach is focus on characterizing not only the storm-scale but also the large-scale unstable modes and their mutual interaction, there are two different scaling factors for these scale modes separately.

In the TK93's breeding extended design for TC predicting (hereafter known as the TC-breeding method or TCB), steps to make the TC-bred seeds as follows:

Step 1: Remove the GFS original vortex and insert a bogus vortex into the GFS initial condition to obtain a new first guess \mathbf{x}^a . In which, the bogus vortex is dynamical constructed based on the observed minimum sea-level pressure and maximum surface wind, using the Australian Bureau of Meteorology's Tropical Cyclone Limited Area Prediction System (TC-LAPS) package. This step is essential due to the weaknesses of the original GFS vortex in coarse resolution;

Step 2: adding and subtract a bred seeds \mathbf{d}_i ($i = 1, 2, \dots, 6$), then we have 6 first guess $\mathbf{x}1_i^a = \mathbf{x}^a + \mathbf{d}_i$ (positive sector) and $\mathbf{x}2_i^a = \mathbf{x}^a - \mathbf{d}_i$ (negative sector)

Step 3: Run 6-hour lead time forecasts for both positive and negative sectors

Step 4: Separate 6-h forecasts (operators \mathbf{S}^m and \mathbf{S}^v) of positive sector ($\mathbf{x}1_i^f$) and negative sector ($\mathbf{x}2_i^f$) from the previous breeding ensemble forecasts into an environmental component $\mathbf{S}^m \mathbf{x}1_i^f$ and $\mathbf{S}^m \mathbf{x}2_i^f$ and a vortex component ($\mathbf{S}^v \mathbf{x}1_i^f$ and $\mathbf{S}^v \mathbf{x}2_i^f$, **Figure 4a**).

Step 5: Find difference (operator \mathbf{H} , **Figure 4a**) of each set of bred vector pairs (or seeds) from previous 6-h cycles to obtain environmental bred vectors

$\mathbf{m}_i = \mathbf{S}^m (\mathbf{p}_i^f - \mathbf{n}_i^f)$ and the TC bred vectors $\mathbf{v}_i = \mathbf{S}^v (\mathbf{p}_i^f - \mathbf{n}_i^f)$;

Step 6: normalize the environmental bred vectors (by using a normalizing operator \mathbf{C}_m) to obtain a new set of normalized bred vector $\mathbf{C}_m \mathbf{m}_i$, then use an orthogonal operator \mathbf{T} to obtain an orthogonal set of environmental bred vectors $\mathbf{TC}_m \mathbf{m}_i$. Here, the environmental re-scaling operator \mathbf{C}^m acting on a vector \mathbf{v} is defined as:

$$\mathbf{C}^m \mathbf{v} \equiv \Lambda \frac{\mathbf{v}}{\|\mathbf{v}\|}, \quad (7)$$

With the scaling factor for the environmental perturbations given by

$$\Lambda = \left[\frac{1}{2\Gamma} \int_D \int_z \left[U'^2 + V'^2 + \frac{C_p}{T} T'^2 \right] dz dS \right]^{\frac{1}{2}}, \quad (8)$$

And the norm $\|\cdot\|$ taken to be the energy norm as follows:

$$\|\mathbf{v}\|^2 = \left[\frac{1}{2\Gamma} \int_D \int_z \left[u'^2 + v'^2 + \frac{C_p}{T_0} T'^2 \right] dz dS \right]^{\frac{1}{2}},$$

where Γ is the normalized factor proportional to the model domain volume, $C_p = 1006 \text{ J kg}^{-1} \text{ K}^{-1}$; $T_0 = 300 \text{ K}$), D is the model domain area after the model vortex was filtered, $U' = V' = 1.8 \text{ ms}^{-1}$, and $T' = 0.7 \text{ K}$. These values are established in the study of Saito et al. [13], which are also consistent with the

previous estimation by Wang and Bishop [60]; Repeat step 6 for the TC bred vectors with operator C_x to obtain a set of orthogonal TC bred vectors $TC_x v_i$.

Step 7. Make a new pairs of breeding members by adding/subtracting the environmental and TC bred components into the analysis x^a , i.e.,

$$x1_i^a = x^a + TC_m m_i + TC_x v_i \text{ and } x2_i^a = x^a - TC_m m_i - TC_x v_i.$$

Step 8: Run 6-hour lead time forecasts of all positive and negative pair to serve as the first guess for the next analysis cycle;

Step 9. Repeat step 1–9 for the next analysis cycle;

Noted that the above steps are taken only for the warm-start mode in which the ensemble breeding forecasts in the analysis procedure has been available since the previous. For the cold start cycle at which the “INVEST” information for a tropical depression is first issued, it is apparent that the bred vectors are unknown yet, therefore the ensemble initialization requires a different procedure.

One can do the cold-start in countless ways, for example using a random Gaussian noise with a prescribed error distribution, or directly use of the global GFS ensemble forecasts. For simplicity, the approach uses the 6-h difference from previous GFS short-range forecasts for all of the cold-start ensembles. This approach, known as lagged-averaged forecasts (LAF) from Kalnay [58], can quickly capture the most unstable modes in the model, thus allowing the breeding ensemble to speed up the dynamically representation to the environment. The combination of these short-range forecasts can generate a predefined number of seeds from which the breeding ensemble can be obtained. Consider, for example, a configuration of the breeding ensemble experiments requires a total of six bred vectors. Those bred vectors are initialized by taking six 6-h differences of the previous -36 h, -24 h, -18 h, -12 h, and -6 h forecasts that are all taken from the cold start ensemble (**Figure 4b**). The control forecast preprocessed directly from the GFS analysis then adds/subtracts the given bred vectors to create an ensemble of total 13 members for subsequent ensemble forecasts.

2.2.1 Example 2

The TC Breeding method has been implemented the Regional Atmospheric Modeling System (RAMS, version 6.0) model to forecast the TC track in the WPAC basin. In this study, the model domain is a region limited by 5°S–35°N and 100–150°E. This domain is sufficiently large to cover most of the tropical cyclone that formed in the WPAC basin and part of the Tibetan plateau that affects the large-scale steering flow of the TC tracks in the WPAC basin. The model integration time is 60s, and the experimental maximum lead times were up to 5 days (120 h). The convection parameterization schemes used among all experiments included a Kuo scheme, a Kain–Fristch scheme (original) and the new Kain–Fristch scheme (modified version). Initial data for model input were taken from the National Center for Environmental Prediction (NCEP) Global Forecast System (GFS) operational forecast with resolution of $1^\circ \times 1^\circ$. A set of 14 tropical cyclones between 2009 and 2011 in the WPAC basin were chosen for testing the TCB method (**Table 1**).

A series of 120 h forecasts for all storms in **Table 1** were conducted, using the aforementioned TC-breeding technique. The retrospective experiments include six positive/negative pairs and a control forecast (total 13 members). Here, the control forecasts are just the integrated results from the RAMS model with initial conditions where the original GFS forecasts adding a bogus vortex to make sure the model storm intensity was equivalent to the reality. The experiments used the default mode of the TC-LAPS package in which the constructed bogus vortex that had the horizontal resolution of $1^\circ \times 1^\circ$, and the isobaric vertical coordinates with 26

No	Name	Start date	End date
2009			
1	CHANHOM	18z02052009	00z09052009
2	LINFA	06z17062009	12z22062009
3	GONI	00z30072009	12z09082009
4	MUJIGAE	12z08092009	00z12092009
5	KETSANA	00z25092009	06z30092009
6	PARMA	18z28092009	18z28092009
7	MIRINAE	18z26102009	12z02112009
2010			
8	CONSON	18z11072010	18z17072010
9	CHANTHU	00z18072010	06z23072010
2011			
10	HAIMA	00z19062011	18z24062011
11	NOCKTEN	06z25072011	15z30072011
12	NESAT	00z24092011	12z30092011
13	NALGAE	00z28092011	06z05102011
14	WASHI	00z15122011	18z19122011

Table 1.
List of storms between 2009 and 2011 in the WPAC basin used in this study.

pressure levels as 1000, 975, 950, 925, 850, 800, 750, 700, 650, 600, 550, 500, 450, 400, 350, 300, 250, 200, 150, 100, 70, 50, 30, 20, and 10 h Pa. The variables to characterize the bogus vortex included sea level pressure (P), horizontal wind components (U, V), temperature (T), geopotential height (H), and relative humidity (RH). The cycles of all breeding ensemble were every 12 h, using the TCB method described above. Besides, for convenience, the domain of storm-scale perturbation was also fixed with enclosing area of 1000 km × 1000 km, centered at the vortex location. Three perturbed state variables in the model at the breeding cycles included the horizontal winds and potential temperature at all pressure levels. These cycles (12-h interval) are suitable enough to capture both the fast-growing weather signals at the micro- to meso- scale and the slower baroclinic modes at larger scales.

Results indicated that TCB method helps reduce the track errors. The improvement is approximately 10% reduction in the track forecast errors at the 4- to 5- day lead times as compared to deterministic forecasts integrated from GFS derived-initial conditions. While the improvement is not significant at shorter lead time (1–3 lead times, **Figure 5**).

Besides, the major difference between this TCB method and the original approach of TK93 is the dissimilarity in treatment of perturbations between large-scale environments and storm-scale inner-core, which are then orthogonalized in different manners. For the environmental perturbations in all experiments, a volume limited by [100–150°E] × [5°S–35°N] × [1000–10 h Pa] is chosen. In facts, the domain size does not have significant impact on the magnitude of EBVs, when it is important for the TBVs in some aspects. That is because storms do not always have a fixed size, thus the use of a predefined domain with a constant radius of 1000 km may not fully characterize the storm-scale TC-like vortex. One can design a suitable

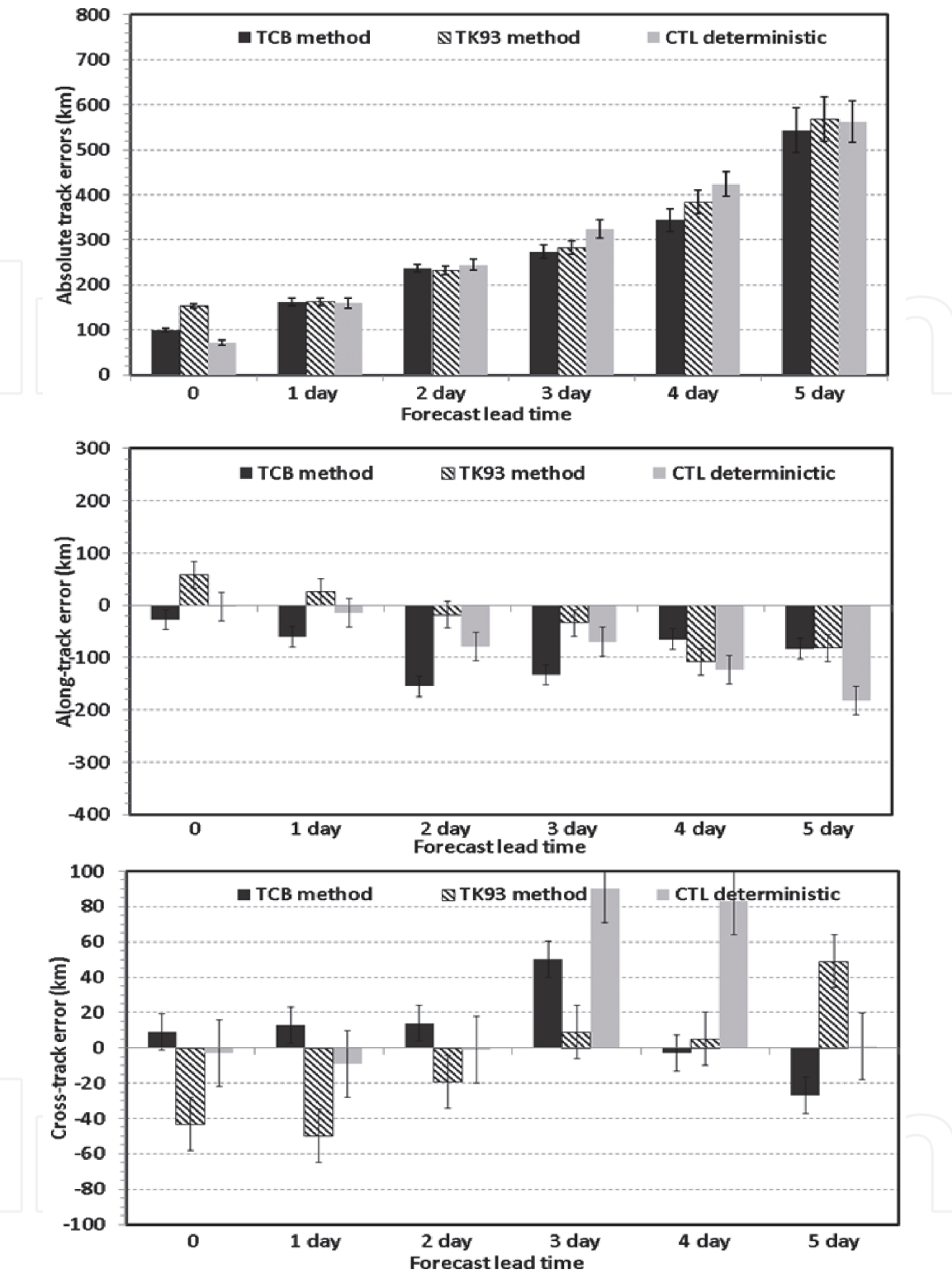


Figure 5. Track forecast distance errors between the TK93’s original breeding ensemble (striped column) forecasts and the deterministic control forecasts (gray columns) for 2009–2011 seasons using the RAMS model [47].

adaptive storm domain to optimize the effectiveness of the TCB method. However, with a coarse resolution of 30 km, the adaptive approach cannot capture the true detailed TC inner-core structure. For more simplicity of the experiment design in this study, the filtering domain has a fixed horizontal radius of 1000 km in all experiments with a warning that this constant size could be a caveat for very broad TCs. It should be noted also that the control analysis would add or subtract the bred vectors, and a potential drift of the control run from the actual states may shift the entire ensemble further from the truth after several cycles. However, with the

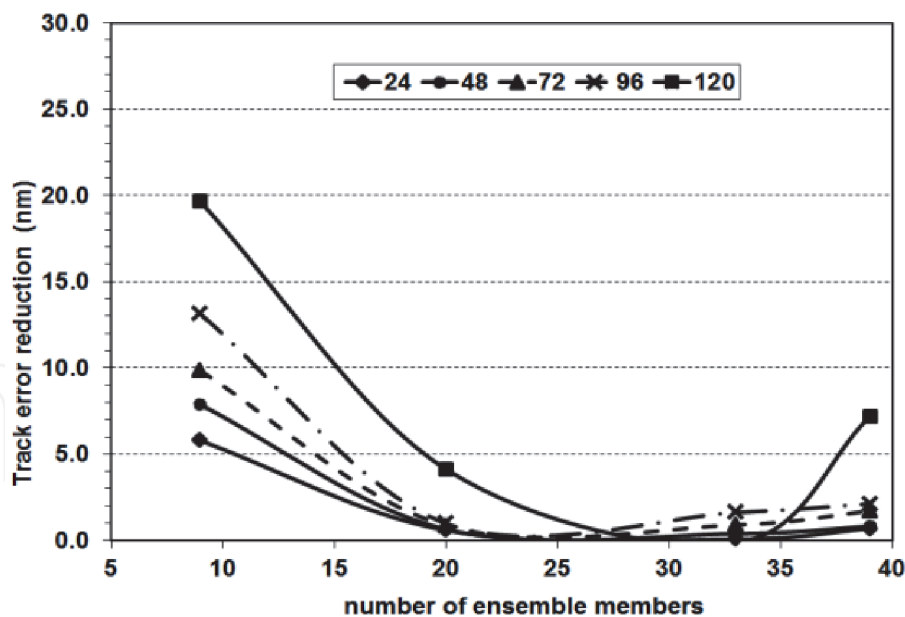


Figure 6.
Rate of track forecast error base on the number of the ensemble members for forecast ranges: The 24-h (diamond), 48-h (circle), 72-h (triangle), 96-h (times), and 120-h (square). The reducing rate is determined as the difference of the track errors when adding newly member to the system at each lead time [56].

integration lead time of only 12 h at each cycle from the control forecast using the GFS forecasts, such a drift is not a big issue and the ensemble thus always maintains their close trajectory to the truth at every initial time.

Sensitivity experiments showed that the best results with ~30 ensemble members are adequate to construct a TCB technique. By gradually increasing the number of ensemble members, the rate of reducing track error per newly added member becomes saturated after reaching the number of 30 ensemble members (**Figure 6**). This saturation of the track errors could link to the maximum information that the orthogonalization of the bred vectors to be obtained after the system reaches its noise level. Otherwise, adding more ensemble member could provide no further benefit to the system, it could even slow down the computation. It should be noted that the 30-km resolution of all ensemble experiments does not fully verify the necessity of separating the treatments for the storm-scale bred vectors and the large-scale bred vectors in distinguished manners. Theoretically, one could design the experiments with higher resolution to further assess the sensitivity of the breeding ensemble technique for more precise experiments, but this would require a large amount of computational and storage resources beyond our current capability. Although this minor problem about resolution, the overall track forecast improvement with the TCB approach suggests that this approach could somehow shed light on ensemble TC track forecast, especially under the circumstances where the observational information is not enough to execute more complex data assimilation steps in real-time forecasting systems.

3. Conclusions

This chapter has presented several techniques to improve the predictive quality of tropical cyclone formation and trajectory. For the forecast of TCs formation, the LETKF algorithm and its implementation in the WRF model and the Vortex tracking method have been introduced. Results in example 1 show that due to a better approach in capturing the real world monsoon trough by assimilating augmented

observations available during the early stages of TC Wutip, the WRF-LETKF model had provided better forecasts about the formation location and timing of typhoon Wutip in comparison to the forecasts that used initial conditions directly from GFS global model. Besides, the results from this study also show the CIMSS-AMV data played a vital role in improving the information of the large-scale environment required for TC formation that one should consider for real-time TC forecasts. For the tropical cyclone track forecasts, a breeding ensemble technique is introduced. This technique is developed based on the original breeding method (TK93). Experiments with 14 TCs (**Table 1**) in **example** showed a promising reduction of track forecast errors by using the TCB technique, especially at 4–5 days forecast range.


However, both the track forecasts by TCB method and the control forecasts are similar in the patterns of cross- and along track forecast errors. This indicated that model inherent errors also are a significant contributor to the track forecast errors that the TCB method is unable to eliminate. Sensitivity experiments of adding gradually each ensemble members exhibit further that the increasing number of members could reduce the track forecast errors, but reduction rate saturates when the number reaches 30 due to the inefficiency of the TCB method in orthogonalizing bred vectors. However, while the TCB method cannot eliminate model inherent errors related to inadequate representation of sub-grid scales when using only parameterizations of physical processes in the RAMS model or the inefficient model resolution, this method could somehow optimize the use of the breeding ensemble technique for tropical cyclone track forecasts in real-time forecasting systems which do not require high computational resources.

Author details

Cong Thanh, Dao Nguyen Quynh Hoa and Tran Tan Tien*
VNU University of Science, Hanoi, Vietnam

*Address all correspondence to: tientt49@gmail.com

IntechOpen

© 2021 The Author(s). Licensee IntechOpen. This chapter is distributed under the terms of the Creative Commons Attribution License (<http://creativecommons.org/licenses/by/3.0>), which permits unrestricted use, distribution, and reproduction in any medium, provided the original work is properly cited. 

References

- [1] Chen J., Lin S., Zhou L., Chen X., Rees S., Bender M., and Morin M.: Evaluation of tropical cyclone forecasts in the next generation global prediction system. *Mon. Wea. Rev.* 2019;147: 3409–3428. DOI: <https://doi.org/10.1175/MWR-D-18-0227.1>
- [2] Zhao M., Held I. M., Lin S.-J., and Vecchi G. A.: Simulations of global hurricane climatology, interannual variability, and response to global warming using a 50-km resolution GCM. *J. Climate*. 2009;22:6653–6678. DOI: <https://doi.org/10.1175/2009JCLI3049.1>
- [3] Chan J. C. L., and Kwok R. H.: Tropical cyclone genesis in a global numerical weather prediction model. *Mon. Wea. Rev.* 1999;127:611–624. DOI: [https://doi.org/10.1175/1520-0493\(1999\)127<0611:TCGIAG>2.0.CO;2](https://doi.org/10.1175/1520-0493(1999)127<0611:TCGIAG>2.0.CO;2)
- [4] Cheung K. K., and Elsberry R. L.: Tropical cyclone formations over the western North Pacific in the Navy Operational Global Atmospheric Prediction System forecasts. *Wea. Forecasting*. 2002;17:800–820. DOI: [https://doi.org/10.1175/1520-0434\(2002\)017<0800:TCFOTW>2.0.CO;2](https://doi.org/10.1175/1520-0434(2002)017<0800:TCFOTW>2.0.CO;2)
- [5] Halperin D. J., Fuelberg H. E., Hart R. E., Cossuth J. H., Sura P., and Pasch R. J.: An evaluation of tropical cyclone genesis forecasts from global numerical models. *Wea. Forecasting*. 2013;28: 1423–1445. DOI: <https://doi.org/10.1175/WAF-D-13-00008.1>
- [6] Halperin D. J., Fuelberg H. E., Hart R. E., Cossuth J. H.: Verification of tropical cyclone genesis forecasts from global numerical models: Comparisons between the North Atlantic and eastern North Pacific basins. *Wea. Forecasting*. 2016;31: 947–955. DOI: <https://doi.org/10.1175/WAF-D-15-0157.1>
- [7] Oouchi K., Yoshimura J., Yoshimura H., Mizuta R., Kusunoki S., and Noda A.: Tropical cyclone climatology in a global warming climate as simulated in a 20 km-mesh global atmospheric model: Frequency and wind intensity analyses. *J. Meteor. Soc. Japan*. 2006;84: 259–276. DOI: <https://doi.org/10.2151/jmsj.84.259>
- [8] Szunyogh I., Kostelich E. J., Gyarmati G., Kalnay E., Hunt B. R., Ott E., Satterfield E., and Yorke J. A.: A local ensemble transform Kalman filter data assimilation system for the NCEP global model. *Tellus*. 2008;60A:113–130. DOI: <https://doi.org/10.1111/j.1600-0870.2007.00274.x>
- [9] Zhou L., Lin S.-J., Chen J.-H., Harris L. M., Chen X., and Rees S.: Toward convective-scale prediction within the Next Generation Global Prediction System. *Bull. Amer. Meteor. Soc.* 2019; 100:1225–1243. DOI: <https://doi.org/10.1175/BAMS-D-17-0246.1>
- [10] Aberson S. D., Aksoy A., Sellwood K. J., Vukicevic T., and Zhang X.: Assimilation of high-resolution tropical cyclone observations with an ensemble Kalman filter using HEDAS: Evaluation of 2008–2011 HWRF forecasts. *Mon. Wea. Rev.* 2015;143: 511–523. DOI: <https://doi.org/10.1175/MWR-D-14-00138.1>
- [11] Holt C., Szunyogh I., Gyarmati G., Leidner S. M., and Hoffman R. N.: Assimilation of tropical cyclone observations: Improving the assimilation of TCVitals, scatterometer winds, and dropwindsonde observations. *Mon. Wea. Rev.* 2015;143: 3956–3980. DOI: <https://doi.org/10.1175/MWR-D-14-00158.1>
- [12] Kieu C. Q., Minh P. T., and Mai H. T.: An application of the multi-physics ensemble Kalman filter to typhoon forecast. *Pure Appl. Geophys.* 2013;171: 1473–1497. DOI: <https://doi.org/10.1007/s00024-013-0681-y>

- [13] Saito K., and Coauthors: The WWRP Beijing Olympic 2008 RD Project. Meeting on the Study of data assimilation and evaluation of forecast reliabilities for dynamical prediction of heavy rainfall. Meteorological Research Institute. Mar 2008, Japan.
- [14] Tong M., and Coauthors: Impact of assimilating aircraft reconnaissance observations on tropical cyclone initialization and prediction using operational HWRF and GSI ensemble-variational hybrid data assimilation. *Mon. Wea. Rev.*. 2018;146;4155–4177. DOI: <https://doi.org/10.1175/MWR-D-17-0380.1>
- [15] Zhang F., and Weng Y.: Predicting hurricane intensity and associated hazards: A five-year real-time forecast experiment with assimilation of airborne Doppler radar observations. *Bull. Amer. Meteor. Soc.*. 2015;96;25–33. DOI: <https://doi.org/10.1175/BAMS-D-13-00231.1>
- [16] Zhang F., Weng Y., Gamache J. F., and Marks F. D.: Performance of convection-permitting hurricane initialization and prediction during 2008–2010 with ensemble data assimilation of innercore airborne Doppler radar observations. *Geophys. Res. Lett.*. 2011;38;L15810. DOI: <https://doi.org/10.1029/2011GL048469>.
- [17] Du T. D., Ngo-Duc T., and Kieu C.: Initializing the WRF Model with tropical cyclone real-time reports using the ensemble Kalman filter algorithm. *Pure Appl. Geophys.*. 2017;174;2803–2825. DOI: <https://doi.org/10.1007/s00024-017-1568-0>.
- [18] Pu Z., Zhang S., Tong M., and Tallapragada V.: Influence of the self-consistent regional ensemble background error covariance on hurricane inner-core data assimilation with the GSI-based hybrid system for HWRF. *J. Atmos. Sci.*. 2016;73;4911–4925. DOI: <https://doi.org/10.1175/JAS-D-16-0017.1>.
- [19] Snyder C., and Zhang F.: Assimilation of simulated Doppler radar observations with an ensemble Kalman filter. *Mon. Wea. Rev.*. 2003;131;1663–1677. DOI: <https://doi.org/10.1175/2555.1>
- [20] Ott E., and Coauthors: A local ensemble Kalman filter for atmospheric data assimilation. *Tellus*. 2004;56A;415–428. DOI: <https://doi.org/10.3402/tellusa.v56i5.14462>
- [21] Hunt B. R., Kostelich E. J., and Szunyogh I.: Efficient data assimilation for spatiotemporal chaos: A local ensemble transform Kalman filter. *Physica D*. 2007;230;112–126. DOI: <https://doi.org/10.1016/j.physd.2006.11.008>.
- [22] Holmlund K., Velden C., and Rohn M.: Enhanced automated quality control applied to high-density satellite-derived winds. *Mon. Wea. Rev.*. 2001;129;517–529. DOI: [https://doi.org/10.1175/1520-0493\(2001\)129<0517:EAQCAT>2.0.CO;2](https://doi.org/10.1175/1520-0493(2001)129<0517:EAQCAT>2.0.CO;2)
- [23] Kang J.-S., Kalnay E., Liu J., Fung I., Miyoshi T., and Ide K.: “Variable localization” in an ensemble Kalman filter: Application to the carbon cycle data assimilation. *J. Geophys. Res.*. 2011;116;D09110. DOI: <https://doi.org/10.1029/2010JD014673>
- [24] Kieu C. Q., Nguyen M. T., Hoang T. M., and Ngo-Duc T.: Sensitivity of the track and intensity forecasts of Typhoon Megi (2010) to satellite-derived atmospheric motion vectors with the ensemble Kalman filter. *J. Atmos. Oceanic Technol.*. 2012;29;1794–1810. DOI: <https://doi.org/10.1175/JTECH-D-12-00020.1>.
- [25] Miyoshi T., and Kunii M.: The local ensemble transform Kalman filter with the weather research and forecasting

model: Experiments with real observations. *Pure Appl. Geophys.* 2012;169;321–333. DOI: <https://doi.org/10.1007/s00024-011-0373-4>.

[26] Cheung K. K. W., Chan J. C. L.: Ensemble Forecasting of Tropical Cyclone Motion Using a Barotropic Model. Part I: Perturbations of the Environment. *Mon. Wea. Rev.* 1999; 127;1229–1243. DOI: [https://doi.org/10.1175/1520-0493\(1999\)127<1229:EFOTCM>2.0.CO;2](https://doi.org/10.1175/1520-0493(1999)127<1229:EFOTCM>2.0.CO;2).

[27] Li H., Kalnay E., Miyoshi T., and Danforth C. M.: Accounting for model errors in ensemble data assimilation. *Mon. Wea. Rev.* 2009;137;3407–3419.

[28] Miyoshi T.: The Gaussian Approach to Adaptive Covariance Inflation and Its Implementation with the Local Ensemble Transform Kalman Filter. *Mon. Wea. Rev.* 2011;139;1519–1535.

[29] Bister M., and Emanuel K. A., 1997: The genesis of Hurricane Guillermo: TEXMEX analyses and a modeling study. *Mon. Wea. Rev.* 1997;125;2662–2682. DOI: [https://doi.org/10.1175/1520-0493\(1997\)125<2662:TGOHGT>2.0.CO;2](https://doi.org/10.1175/1520-0493(1997)125<2662:TGOHGT>2.0.CO;2)

[30] Wen D., Li Y., Zhang D., Xue L., and Wei N.: A statistical analysis of tropical upper-tropospheric trough cells over the western North Pacific during 2006–15. *J. Appl. Meteor. Climatol.* 2018;57;2469–2483. DOI: <https://doi.org/10.1175/JAMC-D-18-0003.1>

[31] Le Marshall J., Rea A., Leslie L., Seecamp R., and Dunn M.: Error characterisation of atmospheric motion vectors. *Aust. Meteor. Mag.* 2004;53; 123–131.

[32] Li J., Li J., Velden C., Wang P., Schmit T. J., and Sippel J.: Impact of rapid-scan-based dynamical information from GOES-16 on HWRF hurricane forecasts. *J. Geophys. Res.*

Atmos. 2020;125;e2019JD031647. DOI: <https://doi.org/10.1029/2019JD031647>

[33] Velden C. S., Hayden C. M., Menzel W. P., Franklin J. L., and Lynch J. S.: The impact of satellite-derived winds on numerical hurricane track forecasting. *Wea. Forecasting*. 1992;7;107–118. DOI: [https://doi.org/10.1175/1520-0434\(1992\)007<0107:TIOSDW>2.0.CO;2](https://doi.org/10.1175/1520-0434(1992)007<0107:TIOSDW>2.0.CO;2)

[34] Velden C. S., Hayden C., Nieman S., Menzel W., Wanzong S., and Goerss J.: Upper-tropospheric winds derived from geostationary satellite water vapor observations. *Bull. Amer. Meteor. Soc.* 1997;78;173–195. DOI: [https://doi.org/10.1175/1520-0477\(1997\)078<0173:UTWDFG>2.0.CO;2](https://doi.org/10.1175/1520-0477(1997)078<0173:UTWDFG>2.0.CO;2)

[35] Tien T. T., Dao N. Q. H., C. Thanh, Kieu C. Q.: Assessing the Impacts of Augmented Observations on the Forecast of Typhoon Wutip's (2013) Formation Using the Ensemble Kalman Filter. *Weather and Forecasting*. 2020; 35;1483–1503.

[36] Cecelski, S. F. and D.-L. Zhang (2013). "Genesis of Hurricane Julia (2010) within an African easterly wave: Low-level vortices and upper-level warming." *J. Atmos. Sci.* **70**: 3799–3817.

[37] Cecelski, S. F., Zhang, D., & Miyoshi, T. (2014). Genesis of Hurricane Julia (2010) within an African Easterly Wave: Developing and Nondeveloping Members from WRF–LETKF Ensemble Forecasts, *Journal of the Atmospheric Sciences*, **71**(7), 2763–2781

[38] Kishimoto K.: JMA's five-day tropical cyclone track forecast. Technical Review No. 12 of the RSMC Tokyo – Typhoon Center. Available online at <http://www.jma.go.jp/jma/jmaeng/jma-center/rsmc-hp-pub-eg/techrev/text12-2.pdf>. 2010.

[39] Zhang Z., and Krishnamurti T. N.: "Ensemble forecasting of hurricane

- tracks." *Bull. Amer. Meteor. Soc.* 1997;78; 2785-2795.
- [40] Elsberry R. L., and Carr III L. E.: Consensus of dynamical tropical cyclone track forecasts—Error versus spread. *Mon. Wea. Rev.* 2000;128;4131–4138. DOI: [https://doi.org/10.1175/1520-0493\(2000\)129<4131:CODTCT>2.0.CO;2](https://doi.org/10.1175/1520-0493(2000)129<4131:CODTCT>2.0.CO;2)
- [41] Kehoe R. M., Boothe M. A., Elsberry R. L.: Dynamical Tropical Cyclone 96- and 120-h Track Forecast Errors in the Western North Pacific. *Wea. Forecasting*. 2007;22;520–538. DOI: <https://doi.org/10.1175/WAF1002.1>
- [42] Tien T. T., C. Thanh, Van H. T., Kieu C. Q.: Two-dimensional retrieval of typhoon tracks from an ensemble of multi-model outputs. *Wea. Forecasting*. 2012;27;451–461.
- [43] Toth Z., Kalnay E.: "Ensemble forecasting at NMC." *Amer. Meteor. Soc.* 1993;74;2317-2330.
- [44] Toth Z., and Kalnay E.: Ensemble forecasting at NCEP and the breeding method. *Mon. Wea. Rev.* 1997;125; 3297–3319.
- [45] Molteni F., Buizza R., Palmer T. N., and Petroliagis T.: "The ECMWF ensemble prediction system: Methodology and validation. ." *Quart. J. Roy. Meteor. Soc.* 1996;122;73-119.
- [46] Palmer T. N., Molteni F., Mureau R., Buizza R., Chapelet P., Tribbia J.: Ensemble prediction. In *Proc. of the ECMWF Seminar on Validation of Models over Europe*. Vol. 1 (ECMWF, Shinfield Park, Reading RG2 9AX, UK). 1993. 285 pp.
- [47] C. Thanh, Tien T. T., and Chanh K. Q.: Application of breeding ensemble to tropical cyclone track forecasts using the regional atmospheric modeling system (rams) model. *Applied Mathematical Modelling*. 2016;40(19–20);8309–8325. DOI: <https://doi.org/10.1016/j.apm.2016.04.010>
- [48] Magnusson L, Kállén E., and Nycander J.: "Initial state perturbations in ensemble forecasting." *Nonlin. Processes Geophys.* 2008;15;751–759.
- [49] Corazza M., Kalnay E., Patil D. J., Ott E., Yorke J., Szunyogh I., Cai M.: Use of the breeding technique in the estimation of the background error covariance matrix for a quasigeostrophic model, in: *AMS Symposium on Observations, Data Assimilation and Probabilistic Prediction*, Orlando, Florida. 2002. pp. 154-157.
- [50] Trevisan A., and Pancotti F.: Periodic orbits, Lyapunov vectors and singular vectors in the Lorenz system. *J. Atmos. Sci.* 1998;55;390-398.
- [51] Annan J. D.: On the orthogonality of bred vectors. *Mon. Weather Rev.*, 2004; 843-849.
- [52] Yang S.-C., Kalnay E., Cai M., Rienecker M., Yuan G., Toth Z.: ENSO Bred Vectors in Coupled Ocean–Atmosphere General Circulation Models. *J. Climate*. 2006;19;1422–1436.
- [53] Legras B., and Vautard R.: A guide to Lyapunov vectors. *Proceedings of the ECMWF Seminar on Predictability*. September 4–8, 1995, Reading, England, Vol 1, ECMWF, Shinfield Park, Reading, UK. 1996. pp. 143-156.
- [54] Vannitsem S., and Nicolis C.: Lyapunov vectors and error growth patterns in a T21L3 quasigeostrophic model. *J. Atmos. Sci.* 1997;54;347-361.
- [55] Black M. L., and Willoughby H. E.: The concentric eyewall cycle of Hurricane Gilbert. *Mon. Wea. Rev.* 1992;120;947–957. DOI: [https://doi.org/10.1175/1520-0493\(1992\)120<0947:TCECOH>2.0.CO;2](https://doi.org/10.1175/1520-0493(1992)120<0947:TCECOH>2.0.CO;2)
- [56] Chen Y., and Yau M. K.: Spiral bands in a simulated hurricane. Part I: Vortex Rossby wave verification. *J.*

Atmos. Sci.. 2001;58;2128–2145. DOI:
[https://doi.org/10.1175/1520-0469](https://doi.org/10.1175/1520-0469(2001)058<2128:SBIASH>2.0.CO;2)
(2001)058<2128:SBIASH>2.0.CO;2

[57] Guinn T. A., and Schubert W. H.:
Hurricane spiral bands. J. Atmos. Sci..
1993;50;3380–3403.

[58] Kalnay E.: "Atmospheric modeling,
data assimilation and predictability",
Cambridge University Press. 2003;512p.

[59] Lorenz E. N.: "The predictability of a
flow which possesses many scales of
motion." Tellus. 1969;21;289-307.

[60] Wang X., Bishop C. H.: A
Comparison of Breeding and Ensemble
Transform Kalman Filter Ensemble
Forecast Schemes. J. Atmos. Sci.. 2003;
60;1140–1158.